

and the 1.63-MeV state are 0.6 ± 0.4 mb/sr and 2.2 ± 0.2 mb/sr, respectively. Morita and Takeshita³⁹ found for 2.17-MeV deuterons that the excited-state yield is about 4 times the ground-state yield at 0° , in agreement with our results.

V. CONCLUSION

The spectrum of neutrons produced by bombardment of Li^7 by 1.98-MeV deuterons gives evidence for only the ground state and well-known 2.9-MeV state in Be^8 below 9-MeV excitation. If other neutron groups are present, their intensity is no more than 10% of that for the ground-state group. These results agree with most measurements on Be^8 . The neutron group to the excited state has a maximum corresponding to 3.1 ± 0.1 MeV excitation and a center-of-mass width of 1.75 ± 0.1 MeV; however, these experimental numbers

³⁹ S. Morita and K. Takeshita, J. Phys. Soc. Japan 13, 1241 (1958).

cannot be interpreted clearly in terms of the parameters for the Be^8 excited state because the spectrum is distorted by the continuum from the three-body decay. It seems that the relative magnitude of the continuum depends on bombarding energy and on the angle of observation. Since a continuum may also accompany other reactions which lead to Be^8 , the level parameters accepted for the purpose of interpreting the spectra are based on the observed phase shifts for α - α scattering rather than on spectra from other reactions. Predictions from the δ_2 phase shifts give a peak width of only 1.3 to 1.4 MeV and a tail which is about half the magnitude of the observed tail.

ACKNOWLEDGMENTS

We wish to thank Dr. Charles Jones for several helpful discussions. C. C. Trail gratefully acknowledges a fellowship with the Oak Ridge Institute of Nuclear Studies which he held while performing these experiments.

Role of Particle-Hole Correlations in the Inelastic Scattering of Electrons from C^{12} , O^{16} , and Ca^{40} †

VINCENT GILLET*

Carnegie Institute of Technology, Pittsburgh, Pennsylvania

AND

MICHEL A. MELKANOFF

University of California, Los Angeles, California

(Received 18 October 1963)

All available experimental data on the inelastic scattering of high-energy electrons from C^{12} , O^{16} , and Ca^{40} have been analyzed in terms of the particle-hole models of nuclear excitations. The calculations do not involve any free parameters. The results proved quite sensitive to the treatment of nuclear correlations and generally favored the random-phase approximation, which yielded satisfactory agreement with most of the data.

I. INTRODUCTION

THE purpose of the present analysis is to determine to what extent the inelastic scattering of electrons from complex nuclei can be used to test the wave functions derived from various extensions of the shell model.

We shall consider the closed-shell nuclei C^{12} , O^{16} , and Ca^{40} wherein the effects of nucleon correlation have been satisfactorily described by two types of approximations.¹⁻³ Approximation I consists in diagonalizing the

effective two-body force in a subspace limited to the configuration of energy $\hbar\omega$. Approximation II has been called the random-phase approximation⁴ (RPA), the quasiboson approximation⁵ and the extended shell-

J. P. Elliott and B. H. Flowers, Proc. Roy. Soc. (London) A242, 57 (1957); S. Fallieros and R. A. Ferrell, Phys. Rev. 116, 660 (1959); G. E. Brown, L. Castillejo, and J. A. Evans, Nucl. Phys. 22, 1 (1961); J. Sawicki and T. Soda, *ibid.* 28, 270 (1961); N. Vinh Mau and G. E. Brown, *ibid.* 29, 89 (1962).

² V. Gillet and N. Vinh Mau, Nucl. Phys. (to be published).

³ V. Gillet and E. Sanderson, Nucl. Phys. (to be published).

⁴ R. A. Ferrell and J. J. Quinn, Phys. Rev. 108, 570 (1957). K. Sawada, K. A. Brueckner, N. Fukuda, and R. Brout, Phys. Rev. 108, 507 (1957); S. Fallieros, Ph.D. thesis, University of Maryland, 1958 (unpublished); G. E. Brown, J. A. Evans, and D. J. Thouless, Nucl. Phys. 24, 1 (1961).

⁵ K. Sawada, Phys. Rev. 106, 372 (1957); R. Arvieu and M. Veneroni, Compt. Rend. 250, 922, 2155 (1960).

† Supported by the National Science Foundation and the Office of Naval Research. Reproduction in whole or in part is permitted for any purpose of the United States Government.

* On leave of absence from Centre d'Etudes Nucléaires de Saclay, France.

¹ W. M. Visscher and R. A. Ferrell, Phys. Rev. 102, 450 (1956);

model approximation⁶; this approximation takes into account some of the effects of excitations of any number of particle-hole pairs in a simple fashion although it admittedly violates the Pauli principle. Both approximations generally yield similar energy spectra except for low-lying $T=0$ states wherein approximation II strongly increases their collective characters and thus helps to improve the over-all agreement with experiment.^{2,3,7} It should be pointed out, however, that the applicability of approximation II to nuclear systems has still not been demonstrated.

Nuclear wave functions obtained in approximations I and II have been found satisfactory in calculating gamma-decay rates,⁸ cross sections for the inelastic scattering of high-energy protons⁹ from C^{12} and alpha particles¹⁰ from Ca^{40} . However, particle scattering calculations require some assumption regarding the interaction between the incident particle and the target nucleus, and this further assumption makes it difficult to evaluate the validity of the nuclear model. On the other hand, the inelastic scattering of high-energy electrons provides a particularly useful tool for testing nuclear models. The interaction between electron and nuclei is known and, in many cases, the first Born approximation is sufficiently accurate considering the nature of shell-model calculations and the uncertainties of presently available experimental data.¹¹ Calculations of inelastic electron scattering have been carried out recently making use of the nuclear wave functions described in Refs. 2 and 3 or similar ones for the $3^- T=0$ and $5^- T=0$ states¹² of Ca^{40} , for the 13-MeV state¹³ of O^{16} , for the low-lying even- and odd-parity states¹⁴ of O^{16} , and for the giant resonance¹⁵ of C^{12} .

In the present article we investigate systematically the model dependence of inelastic electron scattering which excites electric states of C^{12} , O^{16} , and Ca^{40} and for which experimental information is presently available. Most of these states are low-lying ones and have a strongly collective character, therefore their nuclear wave functions are quite sensitive to the model used. We compare the results obtained with the wave functions given by the independent-particle model (IP), approximation I and approximation II. The present calculation does not include any free, adjustable parameter. Indeed, the force parameters were obtained previously by optimizing the fits to the energy spectra⁷ while the harmonic oscillator length parameters are

those which yield the shell-model nuclear charge density required to fit the elastic electron scattering data.¹⁶

Since we are not primarily concerned with obtaining precise fits to the experimental data, we shall follow the simplest treatment of electron scattering, limiting ourselves to the excitation of electric states and describing the interaction solely by means of the longitudinal Coulomb term in the first Born approximation.¹⁷ The Born approximation has been used almost universally and has been shown to be quite adequate within the limitations indicated above.¹⁸ On the other hand, the transverse part of the electric interaction has been shown to be quite negligible for the low-lying collective states with which we shall mainly be concerned.¹⁹

We shall present the radial dependence of the transition density obtained with the above described models for some selected states. This quantity, which completely specifies the nuclear model, has previously been generally assumed to have a simple form peaked at the nuclear surface.²⁰ Such phenomenological forms were adopted by analogy with the static charge densities used in calculating the elastic-scattering form factor.²¹ However, the transition density which is the overlap between the excited- and ground-states wave functions need not be a simple function of r as shown by the present analysis. In many cases we did find that the transition density can resemble a Gaussian curve although its maximum occurs within the nucleus rather than at the nuclear surface. For some excited states characterized by a strong configurational mixing, a Gaussian shape is entirely inadequate as the calculated transition density was found to change its sign. In general, it was found that approximation II yields a better agreement with experimental differential scattering cross sections than approximation I. In particular the results obtained with approximation II for the low-lying 2^+ state of C^{12} and the 3^- state of Ca^{40} are in remarkable agreement with the experiment for moderate values of the momentum transfer. The main difficulty was found for the giant resonance of O^{16} . Although the form factor of the 25.7-MeV state calculated in approximation II agrees satisfactorily with the experiment, the calculated form factors of the 22.6-MeV state are generally too high by a factor of about 2 in all three approximations.

II. THEORY

Most theoretical treatments of inelastic electron scattering have been based on the Born approximation

⁶ M. Baranger, Phys. Rev. **120**, 957 (1960).

⁷ V. Gillet, Nucl. Phys. (to be published).

⁸ E. Boecker (private communication).

⁹ N. Vinh Mau, Ph.D. thesis, University of Paris, 1963 (unpublished).

¹⁰ E. A. Sanderson and N. S. Wall, Phys. Letters **2**, 173 (1962).

¹¹ R. Huby, Rept. Progr. Phys. **21**, 59 (1958).

¹² H. P. Jolly, Jr. (private communication); Phys. Letters **5**, 289 (1963).

¹³ R. S. Willey (private communication).

¹⁴ L. Grünbaum, Ph.D. thesis, Max Planck Institut, Munich, 1963 (unpublished).

¹⁵ F. H. Lewis, Jr., J. D. Walecka, J. Goldemberg, and W. C. Barber, Phys. Rev. Letters **10**, 493 (1963).

¹⁶ L. R. B. Elton, *Nuclear Sizes* (Oxford University Press, Oxford, 1961).

¹⁷ L. I. Schiff, Phys. Rev. **96**, 765 (1954).

¹⁸ T. A. Griffy, D. S. Onley, J. T. Reynolds, and L. C. Biedenharn, Phys. Rev. **128**, 883 (1962).

¹⁹ J. D. Walecka, Phys. Rev. **126**, 663 (1962).

²⁰ Richard H. Helm, Phys. Rev. **104**, 1466 (1956); H. Crannell, R. Helm, H. Kendall, J. Oeser, and M. Yearian, *ibid.* **123**, 923 (1961).

²¹ D. R. Yennie, D. G. Ravenhall, and R. N. Wilson, Phys. Rev. **95**, 500 (1954).

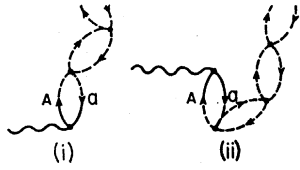


FIG. 1. Representation of nuclear excitation by inelastic electron scattering through (i) creation and (ii) annihilation of a particle-hole pair.

wherein the motion of the electron is described by Dirac plane waves. This leads to the usual description of inelastic differential scattering cross section in terms of form factors.¹¹

$$\sigma(\theta) = \sigma_M(\theta) |F(q(\theta))|^2, \quad (1)$$

where $\sigma_M(\theta)$ is the Mott cross section, i.e., the ultra-relativistic elastic scattering cross section of the electron by a point of charge Ze , and contains most of the kinematics.

$$\sigma_M(\theta) = 4 \left(\frac{Ze^2}{\hbar c} \right)^2 \frac{k_f^2}{q^4(\theta)} \cos^2(\theta/2), \quad (2)$$

where θ is the scattering angle, $q(\theta)$ is the momentum transfer:

$$q^2(\theta) = k_i^2 + k_f^2 - 2k_i k_f \cos\theta,$$

$k_i = E_i/\hbar c$ is the momentum of the incoming electron of energy E_i , while the outgoing electron momentum k_f is given by

$$k_f = (E_i - E^*)/\hbar c, \quad (3)$$

where E^* is the nuclear excitation energy. In Eq. (3) we have neglected the nuclear recoil energy $\hbar^2 q^2/2AM$, where A is the atomic number and M is the proton mass.

If one treats the nucleus nonrelativistically and neglects the transverse electric interaction, the remaining longitudinal Coulomb term yields the following expression¹¹ for the nuclear form factor appearing in Eq. (1).

$$F(q(\theta)) = \langle f | e^{iq(\theta) \cdot r} | i \rangle = 4\pi \sum_{\lambda} \int_0^{\infty} \rho_{if}^{\lambda}(r) j_{\lambda}(qr) r^2 dr. \quad (4)$$

Here $|i\rangle$ is the initial state (the ground state) and $|f\rangle$ the final state of the system. The summation over the multipoles λ is limited by the triangle rule ($J_i J_f \lambda$), where J_i and J_f are the initial and final nuclear spins.

The radial transition density $\rho_{if}^{\lambda}(r)$ defined by Eq. (4) contains all the nuclear information. It is proportional to the reduced matrix element of the one-body operator,

$$O_{\lambda\mu}(r) = \sum_i Y_{\lambda\mu}^*(\theta_i, \varphi_i) \delta(\mathbf{r}_i - \mathbf{r}), \quad (5)$$

where the summation extends over the protons coordinates \mathbf{r}_i . More precisely,

$$\rho_{if}^{\lambda}(r) = \sum_{M_f M_i} \frac{(J_f \lambda M_f M_i | J_i M_i)}{(4\pi)^{1/2} (2\lambda + 1)^{1/2}} \times \langle f | J_f M_f | O_{\lambda\mu}(r) | i | J_i M_i \rangle. \quad (6)$$

In the case of even nuclei with $J_i = 0$, the summation in Eq. (4) is reduced to the term where $\lambda = J_f$ and the form factor $F(q)$ is just the Bessel transform of the transition density $\rho_{if}^{J_f}(r)$.

Two corrections must be introduced into the form factor defined in Eq. (4). First of all the finite size of the proton must be taken into account for large momentum transfers.²² Furthermore, the use of shell-model wave functions which refer to the center of the oscillator well requires a center-of-mass correction.²³ The corrections arising from these effects act in opposite directions and yield a simple factor, multiplying the nuclear form factor

$$f(q) = \exp[-q^2(a_p^2 - 1/\alpha^2 A)/4]. \quad (7)$$

Here a Gaussian form factor has been chosen for the proton with¹³ $a_p^2 = 0.43$ while $\alpha = (M\omega/\hbar)^{1/2}$ is the oscillator well parameter.

Having thus described the scattering process, we now turn to the nuclear problem which is completely contained in the calculation of the radial transition density defined by Eq. (6). It is convenient to express the one-body operator appearing in Eq. (5) in the second quantization representation

$$O_{\lambda\mu}(r) = \sum_{\alpha, \beta} \langle \alpha | O_{\lambda\mu} | \beta \rangle a_{\alpha}^{\dagger} a_{\beta}, \quad (8)$$

where $a_{\alpha}^{\dagger}, a_{\beta}$ are Fermion operators creating or annihilating a nucleon in the single-particle state $|\alpha\rangle = |\alpha j_{\alpha} m_{\alpha}\rangle$ or $|\beta\rangle = |\beta j_{\beta} m_{\beta}\rangle$. If we restrict ourselves to closed-shell nuclei the summation in Eq. (8) will give two types of contributions corresponding to the jump of a particle from a state below the Fermi surface to a state above, and to the drop of a particle from a state above the Fermi surface to an unoccupied state below. In a particle-hole representation where

$$\begin{aligned} \alpha = A \quad \text{and} \quad \beta = a, & \quad \text{if } \epsilon_{\alpha} > \epsilon_F \quad \text{and} \quad \epsilon_{\beta} \leq \epsilon_F, \\ \alpha = a \quad \text{and} \quad \beta = A, & \quad \text{if } \epsilon_{\alpha} \leq \epsilon_F \quad \text{and} \quad \epsilon_{\beta} > \epsilon_F, \end{aligned}$$

these processes correspond to the creation [Fig. 1(i)] or the destruction [Fig. 1(ii)] of a particle-hole pair. The latter process is only possible if such pairs exist in the ground state, i.e., if some of the nucleon correlations in the ground state are taken into account by the nuclear model.

Substituting expression (8) into Eq. (6) for the radial transition amplitude and carrying out the summation over the magnetic quantum numbers,

$$\begin{aligned} \rho_{if}^{\lambda}(r) = \sum_{Aa} \frac{\delta_{\lambda J_f}}{[2(2J_f + 1)]^{1/2}} \varphi_A(r) \varphi_a(r) \\ \times \{ \langle j_A || Y_{\lambda} || j_a \rangle \langle f | a_A^{\dagger} a_a | i \rangle \\ + \langle j_a || Y_{\lambda} || j_A \rangle \langle f | a_a^{\dagger} a_A | i \rangle \}, \quad (9) \end{aligned}$$

where the $\varphi_A(r), \varphi_a(r)$ are oscillator wave functions.

²² R. S. Willey, Nucl. Phys. **40**, 529 (1963).

²³ L. J. Tassie and F. C. Barber, Phys. Rev. **111**, 940 (1958).

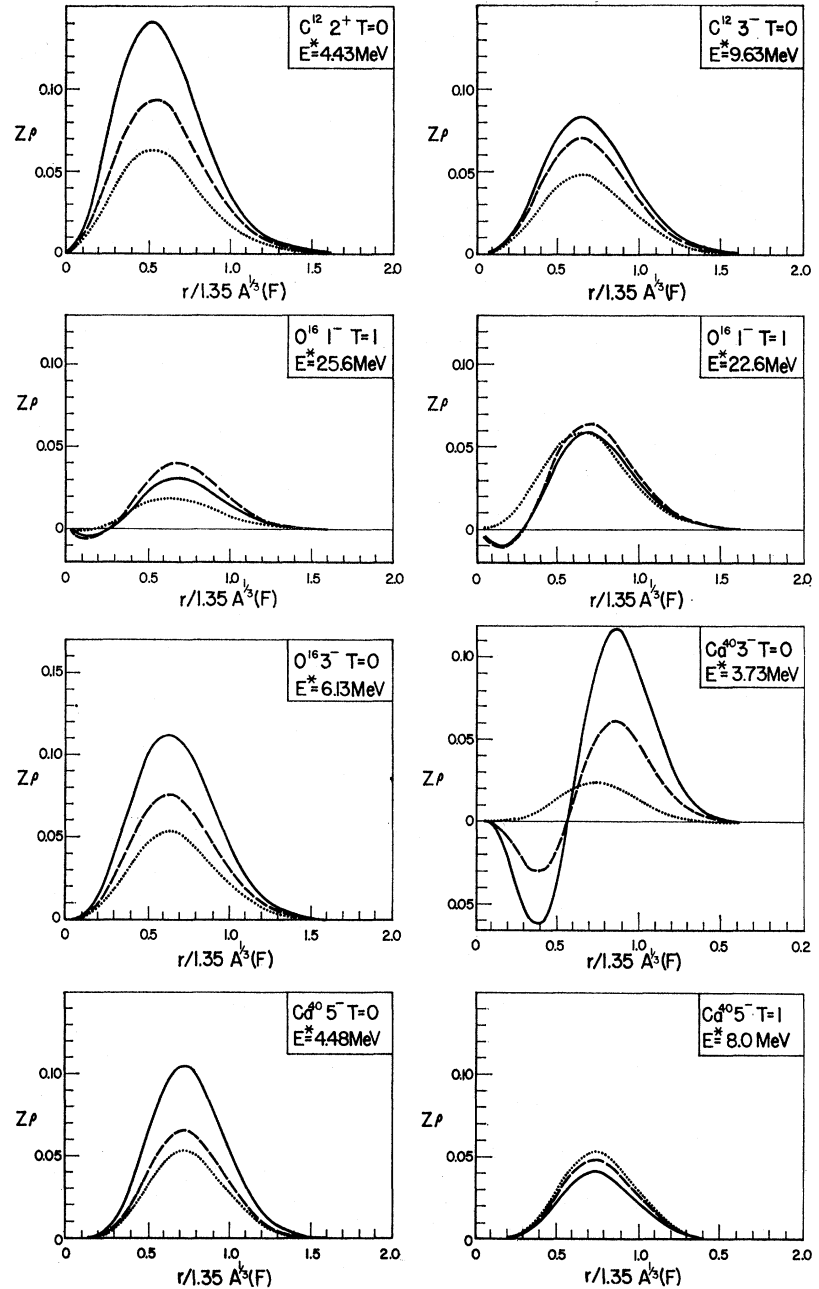


FIG. 2. Radial dependence of the transition densities. Dotted line, IP model; dashed line, approximation I; solid line, approximation II.

The reduced matrix elements of the spherical harmonics $\langle j_A || Y_\lambda || j_a \rangle$, are defined in Edmonds,²⁴ and the $\sqrt{2}$ results from the trivial integration in isotopic spin space. The probability amplitudes, $\langle f | a_a^\dagger a_a | i \rangle$ and $\langle f | a_a^\dagger a_A | i \rangle$, for going from the ground state $|i\rangle$ to the final state $|f\rangle$ by creation or annihilation of the pair (Aa) , are the amplitudes of the particle-hole Green function of the system.²

In the independent-particle model (IP) only one of the amplitudes $\langle f | a_A^\dagger a_a | i \rangle$ will differ from zero.

²⁴ A. R. Edmonds, *Angular Momentum in Quantum Mechanics* (Princeton University Press, New Jersey, 1957).

In approximation I the particle-hole part of the two-body force is diagonalized in the subspace of particle-hole configurations of energy $\hbar\omega$ and one has

$$\begin{aligned} \langle f | a_A^\dagger a_a | i \rangle &= {}_f X_{Aa}^{(I)}, \\ \langle f | a_a^\dagger a_A | i \rangle &= 0, \end{aligned} \quad (10)$$

with the normalization

$$\sum_{Aa} ({}_f X_{Aa}^{(I)})^2 = 1.$$

In approximation II, part of the ground-state correlations are taken into account, permitting annihilation of

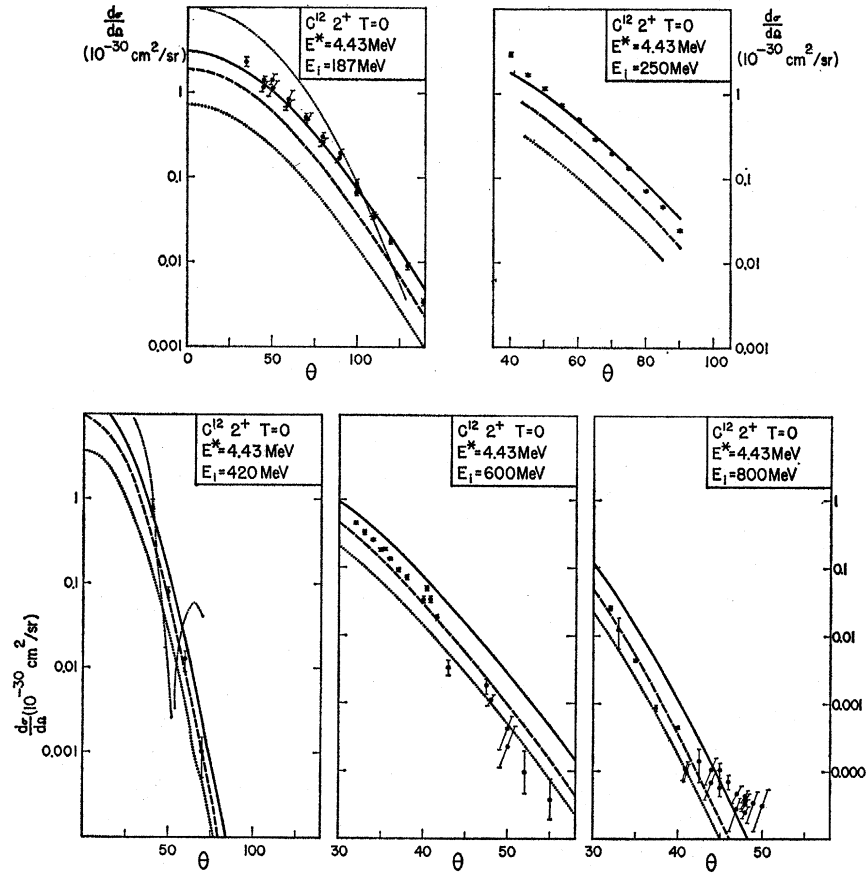


FIG. 3. Differential cross sections for the inelastic scattering of various energy electrons from C^{12} exciting the $2^+ T=0$, 4.43-MeV state. Dotted line, IP model; dashed line, approximation I; solid line, approximation II; dot-dash line, Walecka's curve (Ref. 19). The experimental data is from Refs. 26 and 27.

a particle-hole pair, and

$$\begin{aligned} \langle f | a_A^\dagger a_a | i \rangle &= {}_f X_{Aa}^{(II)}, \\ \langle f | a_a^\dagger a_A | i \rangle &= {}_f Y_{Aa}^{(II)}, \end{aligned} \quad (11)$$

with the special normalization

$$\sum_{Aa} [({}_f X_{Aa}^{(II)})^2 - ({}_f Y_{Aa}^{(II)})^2] = 1.$$

The numerical values of the amplitudes $X_{Aa}^{(I)}$, $X_{Aa}^{(II)}$, and $Y_{Aa}^{(II)}$ used in the present article were taken from Ref. 2 for C^{12} and O^{16} and from Ref. 3 for Ca^{40} . The force parameters which were used to compute the eigenvectors X^I , X^{II} , Y^{II} are those which yielded the best fit to the experimental energy spectra for approximation II.⁷ This choice was motivated by the fact that it was found impossible to fit the $2^+ T=0$ state of C^{12} and the 5^- and 3^- states of Ca^{40} using approximation I.^{2,3} Therefore, the amplitudes used in the present calculation may be expected to somewhat favor approximation II.

As shown by the schematic model,^{25,2} the ${}_f X_{Aa}^{(I)}$ amplitudes have in general the same sign as the one-body matrix element which multiplies them in Eq. (9); accordingly, as one goes from the IP model to approximation I, the transition density given by Eq. (9) is

enhanced. In approximation II, the creation and annihilation amplitudes ${}_f X_{Aa}^{(II)}$ and ${}_f Y_{Aa}^{(II)}$ again have the same sign as the one-body matrix element which multiplies them within a phase factor. This phase factor contributes the same sign to the creation and annihilation term in the $T=0$ states while it contributes opposite signs in the $T=1$ states. Therefore, as one goes from approximation I to approximation II, the transition densities in Eq. (9) should increase in the $T=0$ states, and decrease in the $T=1$ states.

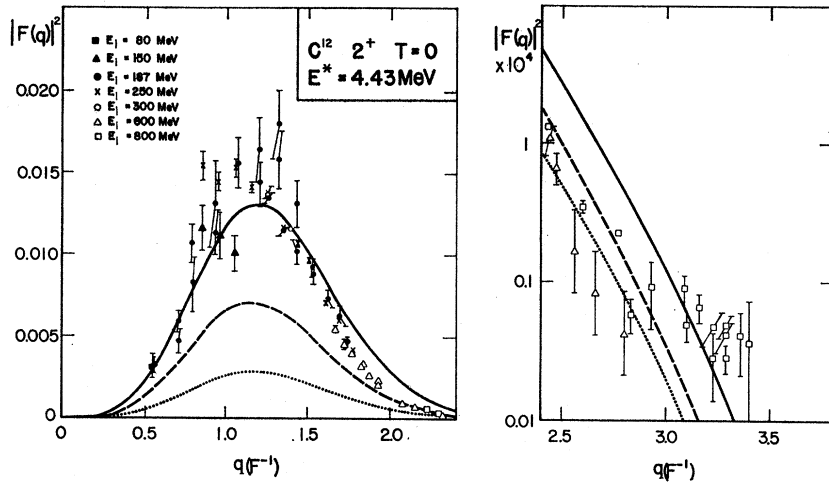
III. RESULTS AND DISCUSSION

A. Transition Densities

In Fig. 2 we present the function $Z\rho(r)$ as a function of the classical nuclear radius for various states of the nuclei C^{12} , O^{16} , and Ca^{40} and for the three models described previously, namely IP model, approximation I and approximation II; the transition charge density is defined by Eq. (6), while Z is the charge number. The abscissa is given in units of the classical nuclear radius $R_0 A^{1/3}$ where A is the mass number and R_0 was chosen as $1.35 F$; this type of scale locates the maximum value of the transition densities with respect to the nuclear surface. The harmonic oscillator parameters α used in the single-particle radial wave functions $\varphi_A(r)$ and $\varphi_a(r)$ entering Eq. (9) are fixed by the analyses of

²⁵ G. E. Brown and M. Bolsterli, Phys. Rev. Letters 3, 472 (1959).

FIG. 4. Form factor of the 2^+ $T=0$, 4.43-MeV state of C^{12} . Dotted line, IP model; dashed line, approximation I; solid line, approximation II. The experimental data is from Refs. 26 and 27.



elastic-electron scattering data according to Ref. 16: $\alpha(C^{12})=0.61 \text{ F}^{-1}$, $\alpha(O^{16})=0.57 \text{ F}^{-1}$, $\alpha(Ca^{40})=0.47 \text{ F}^{-1}$.

The general behavior of the transition density as a function of the model follows the prediction of the schematic model. Thus the introduction of two-body correlations through the use of approximations I and II leads to increased values of ρ as compared with the IP model. This increase in ρ is particularly significant for $T=0$ states. Moreover, the ground-state correlations which are partially brought in by approximation II further increase the value of ρ for $T=0$ states, and decrease it for $T=1$ states as compared to the values of ρ obtained from approximation I.

The radial dependence of the transition density exhibits several interesting features. Generally, the quantities $Z\rho$ have a distinct maximum which almost always occurs at a distance of 50 to 75% of the classical nuclear surface. The transition density corresponding to approximations I and II may change sign as a function of radius. This behavior is particularly pronounced for the octupole state of Ca^{40} for which we have used a mixture of 18 particle-hole configurations³ and, to a lesser extent, for the giant resonances of O^{16} and of C^{12} . The change of sign exhibited by the transition density corresponding to approximations I and II may cause it to

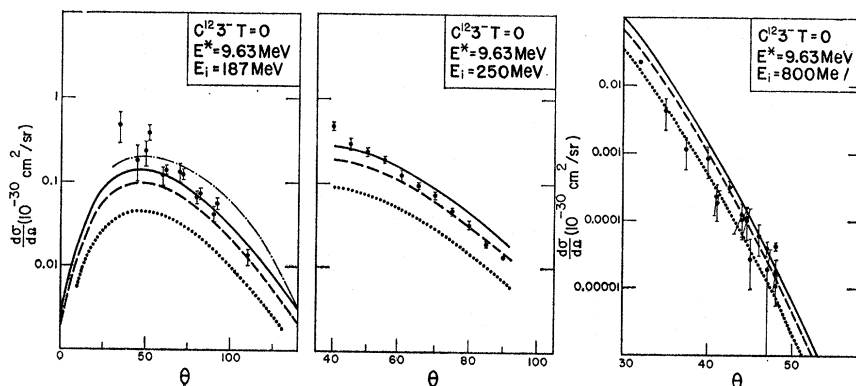
be smaller than that corresponding to the IP model over a certain region of the nucleus; this is particularly noticeable in the case of the 22.5-MeV dipole state of O^{16} for $0.2 < r/(R_0 A^{1/3}) < 0.5$.

The shape of the transition densities shown on Fig. 2 may be contrasted to the phenomenological radial dependence assumed in previous analyses of inelastic electron scattering, namely delta functions, sawtooth, or Gaussian shapes peaked at the nuclear surfaces.^{20,18} Figure 2 shows that although the transition density often resembles a Gaussian curve, it must be peaked well inside the nucleus, which has important consequences since the overlap between the transition density and various Bessel functions determines the form factors. In some cases, such as for the $3^- T=0$ state of Ca^{40} , a simple surface-peaked phenomenological form is totally inadequate.

1. The 2^+ $T=0$ State at 4.43 MeV

The calculated and experimental cross sections for inelastic electron scattering from C^{12} , exciting the 2^+ $T=0$ state, are presented in Fig. 3 for various incident energies. The cross sections calculated with approximation II are in satisfactory agreement with ex-

FIG. 5. Differential cross sections for the inelastic scattering of electrons from C^{12} exciting the $3^- T=0$, 9.63-MeV state. Dotted line, IP model; dashed line, approximation I; solid line, approximation II; dot-dash line, Walecka's curve (Ref. 19). The experimental data is from Refs. 26 and 27.



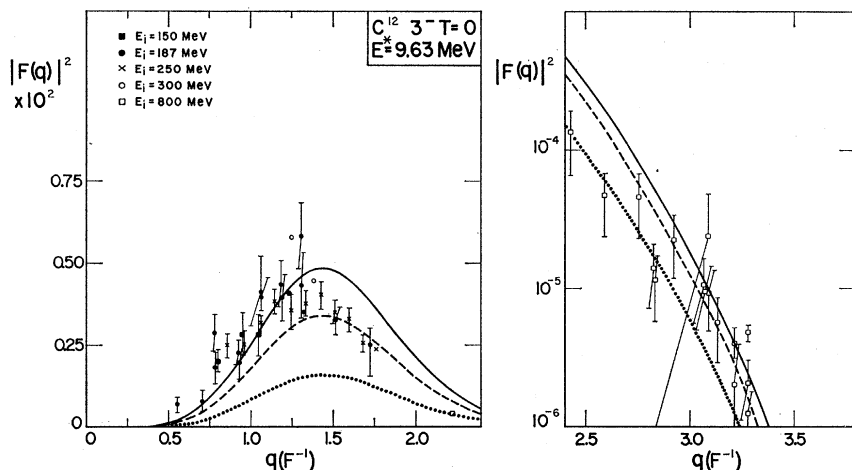


FIG. 6. Form factor for the $3^- T=0$, 9.63-MeV state of C^{12} . Dotted line, IP model; dashed line, approximation I; solid line, approximation II. The experimental data is from Refs. 26 and 27.

periment at 187 and 250 MeV and in fair agreement at 420 MeV. The agreement with experiment is somewhat less satisfactory at 600 and 800 MeV. However, the calculated cross sections become progressively more sensitive to the details of the model as the incident-electron energy increases. This situation can be understood by referring to Eq. (4), which defines the form factor. As the energy of the incident electron increases, the zeros of the Bessel function are shifted towards the center of the nucleus and the function oscillates more violently; thus cancellations occur during the course of the integration in Eq. (4), and errors in the transition densities are magnified in the final results.

The cross section calculated by Walecka¹⁹ by means of an oscillating drop model²⁶ at 187 and 420 MeV are also shown in Fig. 3. It may be seen that the minimum predicted at 50° by this model for $E_i=420$ MeV is not present in the particle-hole models.

All the available experimental data^{19,27,28} at various

energies are summarized in Fig. 4, which presents the form factor, $|F(q)|^2$, as a function of the momentum transfer. The calculated form factors agree with experiment to the same extent as the differential cross section shown in Fig. 3.

2. The $3^- T=0$ State at 9.63 MeV

Figure 5 shows the theoretical and experimental cross section for inelastic scattering of 187-, 250-, and 800-MeV electrons from C^{12} , exciting the $3^- T=0$ state at 9.63 MeV. As in the quadrupole case for 187- and 250-MeV electrons, there is satisfactory agreement between experiment and the results calculated with approximation II. This is somewhat surprising, as it was not possible in Ref. 2 to bring down the calculated energy below 12 MeV in either approximation I or II for any reasonable set of values of the force parameters. This was felt to be a serious discrepancy in view of the over-all success of the particle-hole models in accounting for the energy spectra of the odd-parity states.

Considering the shape of the theoretical curve, it would seem desirable to have experimental points be-

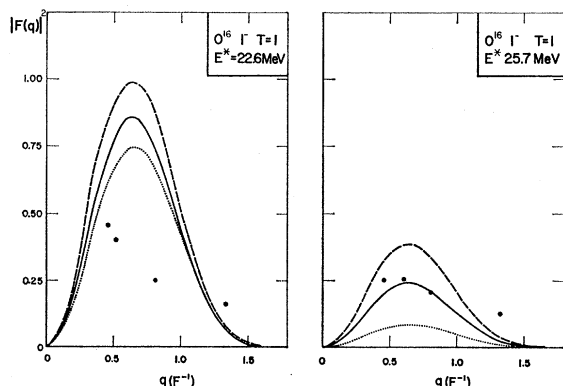


FIG. 7. Form factor for the 22.6- and 25.7-MeV $1^- T=1$ states of O^{16} . Dotted line, IP model; dashed line, approximation I; solid line, approximation II. The experimental data is from Ref. 29.

²⁶ J. D. Walecka, Phys. Rev. **126**, 653 (1962).

²⁷ J. H. Fregeau, Phys. Rev. **104**, 225 (1956); H. F. Ehrenberg, R. Hofstadter, U. Meyer-Berkhout, D. G. Ravenhall, and S. E. Sobottka, *ibid.* **113**, 666 (1959).

²⁸ R. Hofstadter and H. Crannell (private communication).

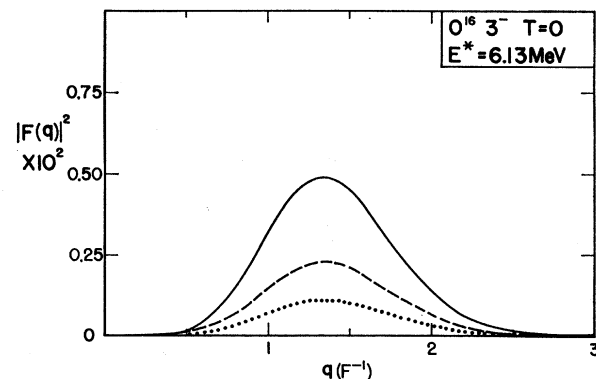


FIG. 8. Form factor for the $3^- T=0$, 6.13-MeV state of O^{16} . Dotted line, IP model; dashed line, approximation I; solid line, approximation II.

TABLE I. Experimental and calculated cross sections for the inelastic scattering of electrons from O^{16} exciting the 22.6- and 25.7-MeV $1^- T=1$ states.

Level	Incident energy E_i (MeV)	Scattering angle θ (deg)	Momentum transfer q (F^{-1})	Experimental cross sections ^a $d\sigma/d\Omega$ (cm^2/sr) $\times 10^{30}$	Theoretical cross sections $d\sigma/d\Omega$ (cm^2/sr) $\times 10^{30}$								
					IP			Approximation I			Approximation II		
					$\alpha=0.51$	$\alpha=0.57$	$\alpha=0.63$	$\alpha=0.51$	$\alpha=0.57$	$\alpha=0.63$	$\alpha=0.51$	$\alpha=0.57$	$\alpha=0.63$
$1^- T=1$ 22.6 MeV	100	60	0.46	1.6	2.41	2.16	1.91	3.27	2.95	2.62	2.81	2.54	2.25
	90	100	0.62	0.185	0.347	0.341	0.323	0.460	0.457	0.437	0.395	0.393	0.375
	150	70	0.81	0.224	0.501	0.578	0.618	0.631	0.746	0.812	0.541	0.640	0.697
	215	80	1.33	0.0397	0.0073	0.0217	0.043	0.0048	0.0204	0.0467	0.0040	0.0174	0.0399
$1^- T=1$ 25.7 MeV	100	60	0.46	0.85		0.228			1.07			0.673	
	90	100	0.61	0.114		0.0369			0.171			0.107	
	150	70	0.81	0.200		0.0641			0.289			0.181	
	215	80	1.32	0.0305		0.0025			0.009			0.0056	

^a See Ref. 29.

low 30° in order to provide a more extensive test of the model.

Experimental data obtained at five different energies are summarized in Fig. 6, which presents experimental and theoretical form factors as a function of q . Again good agreement is obtained between experiment and approximation II as long as the value of q is not too large, i.e., as long as the electrons do not penetrate too deeply into the nucleus.

C. O^{16}

1. The Giant Resonance of O^{16}

Table I presents the available experimental data²⁹ corresponding to excitation of the 22.6- and 25.7-MeV peaks of the giant resonance of O^{16} . The calculated cross sections are also listed for three values of the oscillator well parameter α for the lower peak. The value $\alpha=0.57 F^{-1}$ is obtained by fitting the experimental elastic electron scattering according to Ref. 16. Figure 7 shows the corresponding experimental and theoretical form factors, the latter having been calculated using

$\alpha=0.57 F^{-1}$. It may be seen that the form factors calculated with approximation II are now lower than those calculated with approximation I as expected, since $T=1$.

The form factors and differential scattering cross sections calculated for the higher peak according to approximation II again show generally satisfactory agreement with experiment. Moreover, all three models yield considerably higher values than experiment for the 22.6-MeV peak, and this difficulty cannot be alleviated by a 10% variation in α as indicated in Table I. A similar discrepancy occurs in the case of the radiation widths for which the particle-hole model predicts too high a value as the total-sum rule is only partially exhausted in the giant resonance. The transverse magnetic interaction which has been neglected in the present calculation has been computed for the 22.6-MeV peak by Willey,¹³ who found that the inclusion of this term may significantly increase the form factor for certain values of q ; this would, of course, compound the disagreement with experiment.

2. The $3^- T=0$ State at 6.12 MeV

The form factors for the $3^- T=0$, 6.12-MeV state of O^{16} are plotted on Fig. 8 for the three models. As may be seen, the form factors computed with approximation II are significantly higher than those computed in approximation I. No experimental data is presently available for this state.

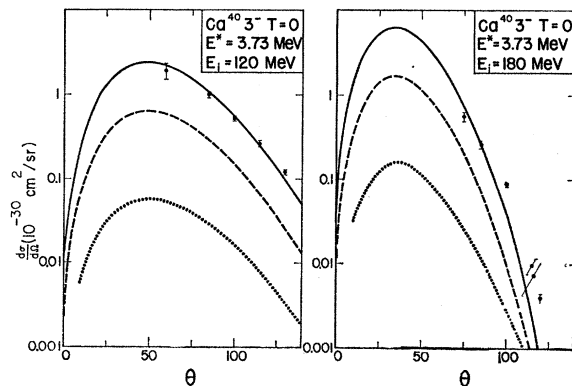


FIG. 9. Differential cross sections for the inelastic scattering of 120- and 180-MeV electrons from Ca^{40} exciting the $3^- T=0$, 3.76-MeV state. Dotted line, IP model; dashed line, approximation I; solid line, approximation II. The experimental data is from Ref. 30.

²⁹ D. B. Isabelle and G. R. Bishop, *J. Phys. Radium* **22**, 548 (1961); D. B. Isabelle, Ph.D. thesis, University of Paris, 1962 (unpublished), and (private communication); D. B. Isabelle and G. R. Bishop, *Nucl. Phys.* **45**, 209 (1963).

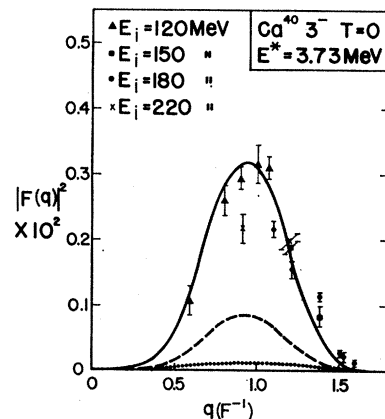


FIG. 10. Form factor for the $3^- T=0$, 3.73-MeV state of Ca^{40} . Dotted line, IP model; dashed line, approximation I; solid line, approximation II. The experimental data is from Ref. 30.

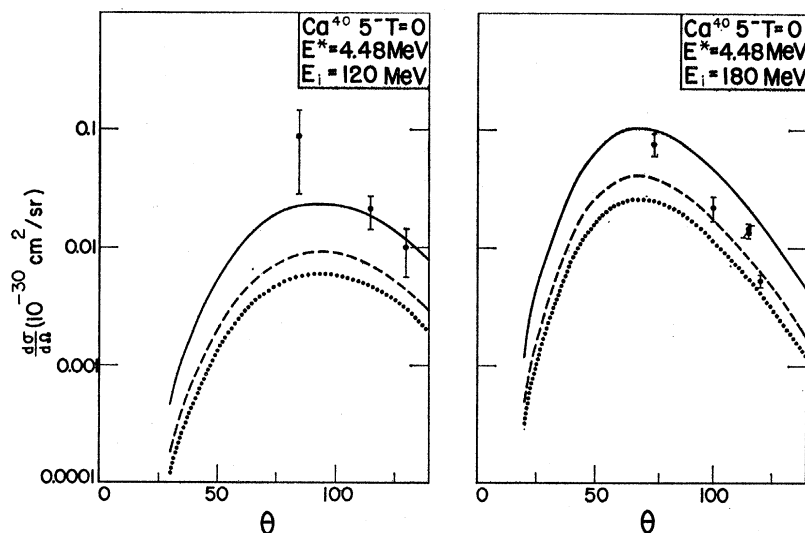


FIG. 11. Differential cross sections for the inelastic scattering of 120- and 180-MeV electrons from Ca^{40} exciting the $5^- T=0$, 4.48-MeV state. Dotted line, IP model; dashed line, approximation I; solid line, approximation II. The experimental data is from Ref. 30.

D. Ca^{40}

1. The $3^- T=0$ State at 3.73 MeV

The differential cross sections for inelastic scattering of 120- and 180-MeV electrons from Ca^{40} , exciting the $3^- T=0$, 3.73-MeV state, are plotted on Fig. 9. It may be seen that the results obtained with approximation II are in striking agreement with experiment³⁰ for 120-MeV electrons and still give satisfactory agreement with experiment for 180-MeV electrons. It should be noted that in this case the transition densities obtained for approximations I and II, shown in Fig. 2, are markedly different from the phenomenological Gaussian shapes often used in previous calculation.

All available data obtained at Orsay and Saclay³⁰ between 120 and 220 MeV are summarized in the form factors presented in Fig. 10, which also includes the calculated form factors for all three models. This figure exhibits the strong increase in the form factors required

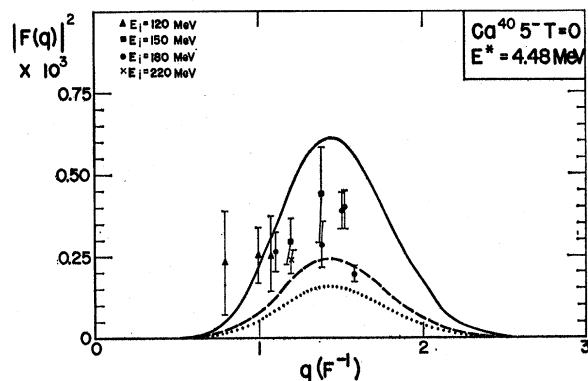


FIG. 12. Form factor for the $5^- T=0$, 4.48-MeV state of Ca^{40} . Dotted line, IP model; dashed line, approximation I; solid line, approximation II. The experimental data is from Ref. 30.

³⁰ D. Blum, P. Barreau, and J. Bellicard, Phys. Letters 4, 109 (1963); J. Bellicard (private communication).

by the data over the values computed from the IP model and approximation I, and achieved by approximation II.

2. The $5^- T=0$ State at 4.48 MeV

The differential scattering cross sections and form factors for inelastic electron scattering from the $5^- T=0$, 4.48-MeV state of Ca^{40} are shown on Figs. 11 and 12. The experimental cross sections³⁰ at 120 MeV seem to favor approximation II. At 180 MeV the experimental cross sections³⁰ fall between the values obtained from approximations I and II and do not permit drawing any definite conclusions.

3. The $5^- T=0$ State at 8 MeV

The particle-hole model of nuclear excitations predicts the existence of a $5^- T=1$ state at about 8 MeV,³

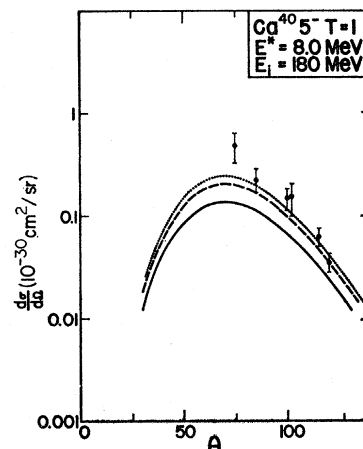


FIG. 13. Experimental differential cross section for the inelastic scattering of 120-MeV electrons from Ca^{40} exciting the 8.0-MeV state, and theoretical values for the lowest $5^- T=1$ state. Dotted line, IP model; dashed line, approximation I; solid line, approximation II. The experimental data is from Ref. 30.

while the electron scattering experiments carried out at Orsay and Saclay show the presence of an excited state at 8.5 MeV.³⁰ Interpretation of the data using Helm's folded charge distribution²⁰ suggests that the excited state should be assigned a J value of 5.³⁰ We compare these experimental cross section and form factors with the predictions of the three models in Figs. 13 and 14. The experimental cross sections are always somewhat greater than the calculated cross sections for all three models, and this suggests that other states may be excited in addition to the $5^- T=1$ state. Such a conclusion is supported by the behavior of the form factors which do not exhibit the usual falloff as q decreases. A similar conclusion was reached by the authors of Ref. 30; recent (α, α') experiments³¹ have also indicated the presence of several odd-parity states between 8 and 9 MeV.

IV. CONCLUSION

In the course of the analysis it was found that the calculated cross sections for high-energy inelastic electron scattering from closed-shell nuclei are sensitive functions of the model used to describe nucleon-nucleon correlation. Despite a simplified treatment of the electron-nuclei interaction and the usual limitations of shell-model calculations, satisfactory agreement has generally been achieved between the experimental data on inelastic electron scattering and the results obtained from approximation II without recourse to any adjustment of parameters. The strong increase in the cross section and form factors, achieved by the introduction of approximation II for the low-lying $T=0$ states, brings the theory into satisfactory agreement with experiment for the $2^+ T=0$ and $3^- T=0$ states of C^{12} and the $3^- T=0$ state of Ca^{40} , while fair agreement is obtained for the $5^- T=0$ state of Ca^{40} . On the other hand, the decrease in the calculated quantity due to the use of approximation II for the $T=1$ states brings the theory into agreement with experiment for the higher peak of the giant resonance of O^{16} , but a serious unexplained discrepancy occurs for all three models in the 22.6-MeV peak. The

³¹ B. Harvey, E. Rivet, and A. Springer (private communication).

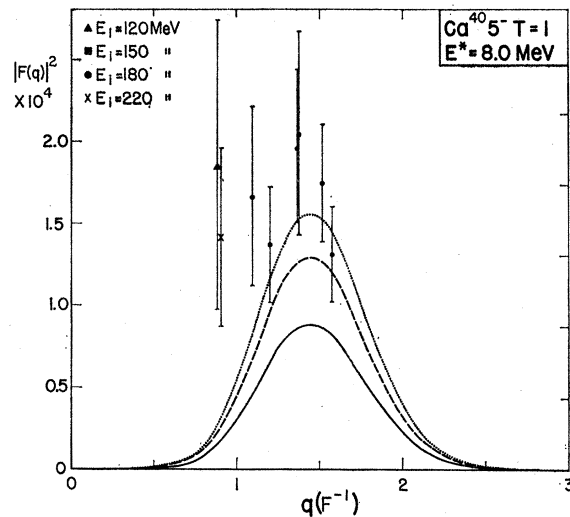


Fig. 14. Experimental form factor for the 8.0-MeV state of Ca^{40} and theoretical values for the lowest $5^- T=1$ state. Dotted line, IP model; dashed line, approximation I; solid line, approximation II. The experimental data is from Ref. 30.

8.5-MeV peak found in Ca^{40} cannot be completely explained by either of the three models assuming the sole excitation of the $5^- T=1$ state predicted by the particle-hole model.

ACKNOWLEDGMENTS

The authors wish to express their gratitude to Professor R. Hofstadter, J. Bellicard, H. Crannell, D. B. Isabelle, and G. R. Bishop for communicating their experimental results prior to publication, and to L. Grünbaum, P. Jolly, and R. S. Willey for communicating the results of their calculations prior to publication. The authors also wish to thank Professor M. Baranger for his interest and for his comments about the present work.

The authors gratefully acknowledge the use of the UCLA IBM-7090 computer. Finally, one of us (V.G.) wishes to acknowledge the hospitality of the Physics Division at the Aspen Institute for Humanistic Studies where part of this work was performed.